# Linkage between Cooperative Oxygenation and Subunit Assembly of Cobaltous Human Hemoglobin†

Michael L. Doyle,‡ Phil C. Speros,§ Vince J. LiCata,§ David Gingrich,∥ Brian M. Hoffman,∥ and Gary K. Ackers*,‡

*Department of Biochemistry and Molecular Biophysics, Washington University School of Medicine, St. Louis, Missouri 63110, Departments of Chemistry and of Biochemistry, Molecular and Cell Biology, Northwestern University, Evanston, Illinois 60201, and Department of Biology, The Johns Hopkins University, Baltimore, Maryland 21218*

*Received February 21, 1991; Revised Manuscript Received April 9, 1991*

ABSTRACT: The thermodynamic linkage between cooperative oxygenation and dimer–tetramer subunit assembly has been determined for cobaltous human hemoglobin in which iron(II) protoporphyrin IX is replaced by cobalt(II) protoporphyrin IX. The equilibrium parameters of the linkage system were determined by global nonlinear least-squares regression of oxygenation isotherms measured over a range of hemoglobin concentrations together with the deoxygenated dimer–tetramer assembly free energy determined independently from forward and reverse reaction rates. The total cooperative free energy of tetrameric cobalt hemoglobin (over all four binding steps) is found to be 1.84 (±0.13) kcal, compared with the native ferrous hemoglobin value of 6.30 (±0.14) kcal. Detailed investigation of stepwise cooperativity effects shows the following: (1) The largest change occurs at the first ligation step and is determined on model-independent grounds by knowledge of the intermediate subunit assembly free energies. (2) Cooperativity in the shape of the tetrameric isotherm occurs mainly during the middle two steps and is concomitant with the release of quaternary constraints. (3) Although evaluation of the pure tetrameric isotherm portrays identical binding affinity between the last two steps, this apparent noncooperativity is the result of a "hidden" oxygen affinity enhancement at the last step of 0.48 (±0.12) kcal. This quaternary enhancement energy is revealed by the difference in subunit assembly free energies of the triply and fully ligated species and is manifested visually by the oxygenation isotherms at high versus low hemoglobin concentration. (4) Cobaltous hemoglobin dimers exhibit apparent anticooperativity of 0.49 (±0.16) kcal (presumed to arise from heterogeneity of subunit affinities). The distribution of cooperative switching effects found in this study is compared with those of ferrous hemoglobin oxygenation and the cobaltous hemoglobin iron–carbon monoxide ligand analogue system [Speros, P. C., Licata, V. J., Yonetani, T., & Ackers, G. K. (1991) *Biochemistry* (preceding paper in this issue)]. The three systems exhibit a common pattern of cooperative switching effects.

Cooperative oxygen binding by human hemoglobin is a thermodynamic property of the macromolecule arising from regulatory interactions between subunits. Intimately related to the regulation of oxygen affinity is the $O_2$-linked dissociation of $(\alpha\beta)_2$ tetramers into $\alpha\beta$ dimers (Ackers & Halvorson, 1974) as shown in Scheme I, where bound oxygen is denoted by X (see Theory for definitions). The changes in stepwise oxygen binding free energies for the tetramer ($\Delta G_{4i}$) are seen to parallel the corresponding differences in dimer–tetramer assembly free energies ($^i\Delta G_2$). Resolution of the equilibrium parameters in the linkage scheme (Scheme I) is therefore of fundamental importance in dissecting the subunit–subunit energetics that regulate oxygen affinity.

Previous studies directed toward this goal have focused on native $HbA_0$[1] (Mills et al., 1976) as a function of the chemical potentials of protons, NaCl, and 2,3-diphosphoglycerate (Chu et al., 1984; Turner, 1984), as a function of temperature (Mills & Ackers, 1979a), and with the mutant hemoglobin Kansas (Atha et al., 1979). In this paper we extend those studies to oxygenation of cobaltous hemoglobin, where the native iron(II) protoporphyrin IX has been replaced by cobalt(II) protoporphyrin IX (Hoffman & Petering, 1970).

Scheme I

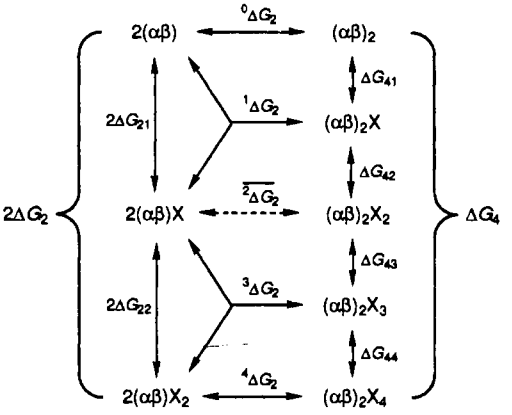


Extending this approach to the oxygenation of CoHb plays a pivotal role in understanding the relationships between oxygenation properties of normal hemoglobin and the energetics of metal-substituted ligand analogue systems. From one perspective the functional consequences of metal substitution at the heme site are determined by comparison with the FeHb oxygenation system (Mills et al., 1976; Chu et al., 1984).

† This work was supported by NIH Grants R37-GM24486, HL13531, and PO1-HL40453 and NSF Grant DMB 86-15497.

* Correspondence should be addressed to this author.
‡ Washington University School of Medicine.
§ The Johns Hopkins University.
∥ Northwestern University.

[1] Abbreviations: CoHb, cobaltous human hemoglobin; Fe–CO, ligand analogue, iron(II)–carbon monoxide, for binding to CoHb; FeHb, ferrous human hemoglobin; $HbA_0$, major component of human hemoglobin; $Na_2EDTA$, disodium ethylenediaminetetraacetic acid; Tris, tris(hydroxymethyl)aminomethane.

0006-2960/91/0430-7263$02.50/0 

From another perspective the present study permits evaluation of the functional consequences of employing Fe–CO as a ligand analogue of $O_2$ by comparison with the cooperative free energies of the 10 CoHb/Fe–CO ligation microstates (Speros et al., 1991). A central question which these studies address is the following: are all these ligation systems operating by a common mechanism, or does the metal substitution lead to a molecule with a new set of cooperativity rules?

## Materials and Methods

*Preparations.* Cobaltous hemoglobin was prepared as described previously (Hoffman & Petering, 1970). Purification was done by HPLC on a Beckman SP-5PW ion-exchange column and shown to be homogeneous by analytical isoelectric focusing. Human haptoglobin was purified by the method of Connell and Shaw (1961).

All kinetic and equilibrium studies were performed in 0.1 M Tris, 0.1 M NaCl, and 1 mM $Na_2EDTA$, pH 7.40, and at 21.50 °C. Reduction enzymes, which are normally used to minimize oxidation of FeHb, were unnecessary because of the stability of CoHb against oxidation.

*Kinetic Determination of* ${}^0K_2$. The dimer–tetramer assembly equilibrium of deoxygenated hemoglobin greatly favors the tetramer form and therefore must be determined by measuring the forward and reverse reaction rates as follows: ${}^0K_2 = k_f/k_r$. The general methods for measuring these reaction rates have been detailed elsewhere (Ip et al., 1976; Turner et al., 1981) and will be discussed only briefly here.

*Dissociation Rate Using Haptoglobin Quenching.* Human haptoglobin binds the dimer form of hemoglobin very rapidly and is essentially irreversible (Nagel & Gibson, 1971; Hwang & Greer, 1980). The rate-limiting process for reacting haptoglobin with tetrameric hemoglobin is dissociation of tetramers to dimers and may be monitored either as an absorbance change of the hemoglobin molecule or as fluorescence quenching of haptoglobin in the haptoglobin–dimer complex (Ip et al., 1976). The pseudo-first-order reaction progress is described by

$$A(t) = A_\infty + P_1 e^{-k_r t} \quad (1)$$

where $A(t)$ and $A_\infty$ are the absorbance values at time $t$, $P_1$ is the amplitude, and $k_r$ is the dissociation rate constant. Separate anaerobic solutions of CoHb and haptoglobin were prepared, and the dissociation reaction was initiated by mixing in a gas-tight split-cell cuvette. The absorbance change for the dissociation reaction was monitored at 401 nm with a Cary 219 spectrophotometer. The reaction was followed on a fast time scale at 401 nm with a Biologic/Molecular Kinetics stopped-flow spectrophotometer. Stoichiometric titrations of FeHb and CoHb with haptoglobin showed the haptoglobin binding reactions to be equally proficient.

The rate of dissociation of tetrameric CoHb into dimers was also monitored as the quenching of fluorescence of the haptoglobin–dimer complex by using the Biologic/Molecular Kinetics instrument. Emission was monitored above 310 nm through a Corning 0160 CS 0-54 filter. Maintenance of anaerobicity was achieved with 0.01% sodium dithionite for the stopped-flow experiments, while an oxygen-scavenging enzyme system was used (Oxyrase, Oxyrase Inc.) for the Cary 219 experiments.

*Reassociation Rate upon Rapid Deoxygenation.* Oxygenated hemoglobin in solution at micromolar concentrations exists as an approximately equal-mass mixture of dimeric and tetrameric forms. Upon rapid deoxygenation a net assembly of dimers into tetramers occurs according to the following bimolecular rate law:

$$A(t) = \frac{A_\infty - A_0}{1 + D_0 k_f t} \quad (2)$$

Here the initial absorbance, final absorbance, and absorbance at time $t$ are $A_0$, $A_\infty$, and $A(t)$, respectively. The initial concentration of dimers is $D_0$, and the forward rate constant is $k_f$. Equation 2 shows that the total amplitude of the reaction ($A_0 - A_\infty$) is a function of $D_0$, and thus the validity of the bimolecular reaction process was substantiated by measuring the reaction at different Hb concentrations. The rate of dimer to tetramer assembly was monitored at 401 nm with a Biologic/Molecular Kinetics stopped-flow system upon rapid deoxygenation with 0.1% sodium dithionite.

*Oxygenation.* Oxygen binding isotherms were measured with either an apparatus based on the design of Imai [Imai, 1978; see Chu et al. (1984)] or the thin-layer cell of Gill (Dolman & Gill, 1978). The Imai method was used for measurements made at protein concentrations less than 600 μM in CoHb monomer because of its long optical path length (2.5 cm), whereas the Gill technique was used at higher protein concentrations because of its short path length (typically 0.005 cm).

The CoHb sample in the Imai cell was equilibrated against 1 atm of humidified oxygen. The oxygen activity was monitored by a Beckman 39065 $O_2$ probe and diminished by flushing the stirred sample with humidified nitrogen gas ($O_2$-free grade, Linde Gases). The linearity of the $O_2$ probe was verified with certified gas mixtures (Linde Gases) of $O_2$ in $N_2$ ($O_2$ percentages were as follows: 0.0075, 0.050, 1.0, 3.50, and 20.95). The fractional saturation of CoHb with $O_2$ was monitored with a Cary 118C spectrophotometer. Absorbance measurements were found to be linear at 450 nm up to approximately 2 absorbance units using gravimetric dilutions of chromate in 0.1 M NaOH (Haupt, 1952). Absorbance values never exceeded 1 absorbance unit in the present study. Temperature was regulated with a Lauda K-2/R water bath to a precision of ±0.02 °C. The precision and accuracy of the temperature in the sample cell were measured with a National Bureau of Standards calibrated thermistor probe/Cole-Parmer 8502-20 digital thermometer. The $pO_2$–absorbance data were measured as voltages in equal increments of time (1 s per point) by using a dual-channel Nicolet Model 3091 digital oscilloscope. Typical deoxygenation times for cobaltous Hb were 45 min. The data were plotted on 8 × 11 paper as absorbance versus logarithm $O_2$ molarity and digitized with a Hewlett Packard 9111a graphics tablet in equal increments of the logarithm $O_2$ molarity.

The thin-layer technique of Gill was operated by equilibrating the sample with 1 atm of humidified $O_2$(g), followed by successive logarithmic dilutions of $pO_2$(g) by means of a precision gas dilution valve. The error in $pO_2$ at each dilution step is not worse than 0.1% relative error (as estimated with an $O_2$ electrode which is only precise to 0.1%). Upon each dilution step a change in absorbance is proportional to the change in fractional saturation. The thin-layer cell is normally operated as a derivative technique, whereby changes in absorbance are measured (Doyle et al., 1990), but was operated in the present study as a continuous method by measuring absolute absorbancies. The continuous mode was chosen solely to allow implementation of a less laborious, microcomputer-controlled data acquisition system.

*Theory.* The linkage between oxygenation of hemoglobin and dimer-tetramer assembly is displayed in Scheme I. Free energy changes are adjacent to arrows which indicate the pertinent equilibria. The process designated by the horizontal dashed arrow represents assembly of doubly ligated tetramer

from: (1) two singly ligated dimers and (2) an unligated dimer and a doubly ligated dimer. For the case of noncooperative[2] $O_2$ binding by dimers, the term ${}^2\Delta G_2$ represents an average equilibrium parameter over each of these reactions (Ackers & Halvorson, 1974).

Free energy changes for binding the $i$th oxygen to dimers ($\Delta G_{2i}$) or tetramers ($\Delta G_{4i}$) are defined by stepwise equilibrium constants as

$$k_{2i} = \frac{[DX_i]}{[DX_{i-1}][X]} \qquad i = 1, 2 \tag{3}$$

for dimers and as

$$k_{4i} = \frac{[TX_i]}{[TX_{i-1}][X]} \qquad i = 1, 2, 3, 4 \tag{4}$$

for tetramers. The product binding constants are given by

$$K_{2i} = \frac{[DX_i]}{[D][X]^i} = \prod_{j=1}^{i} k_{2j} \qquad i = 1, 2 \tag{5}$$

for dimers and

$$K_{4i} = \frac{[TX_i]}{[T][X]^i} = \prod_{j=1}^{i} k_{4j} \qquad i = 1, 2, 3, 4 \tag{6}$$

for tetramers. The total free energy change for binding four oxygens to the tetramer or two oxygens to the dimer is $\Delta G_4$ and $\Delta G_2$, respectively (Scheme I). Dimer–tetramer assembly equilibrium constants are defined for each ligation state of the tetrameric species with $i$ ligands bound as

$${}^iK_2 = \frac{[TX_i]}{[DX_j][DX_k]} \tag{7}$$

where $j + k = i$ and $j, k = 0, 1, 2$.

The fractional saturation, $\bar{Y}$, of the system in Scheme I is an explicit function of seven independent parameters as well as the protein concentration $[P_t]$ (molarity, monomer units) and the ligand activity $X$:

$$\bar{Y} = \frac{Z'_2 + Z'_4\{\sqrt{(Z_2)^2 + 4{}^0K_2Z_4[P_t]} - Z_2\}/\{4Z_4\}}{Z_2 + \sqrt{(Z_2)^2 + 4{}^0K_2Z_4[P_t]}} \tag{8}$$

where

$$Z_2 = 1 + K_{21}[X] + K_{22}[X]^2$$

$$Z'_2 = K_{21}[X] + 2K_{22}[X]^2$$

$$Z_4 = 1 + K_{41}[X] + K_{42}[X]^2 + K_{43}[X]^3 + K_{44}[X]^4$$

$$Z'_4 = K_{41}[X] + 2K_{42}[X]^2 + 3K_{43}[X]^3 + 4K_{44}[X]^4$$

The median ligand activity of an isotherm, $\bar{X}$, is a fundamental thermodynamic quantity which gives the chemical work for complete saturation of the macromolecule [cf. Wyman and Gill (1990)]. It is found as the ligand activity where the areas above and below the isotherm are equal. The median for ligand-linked dimerizing systems is a function of the protein concentration, $[P_t]$, and is a function of the overall linkage parameters: $K_{44}$, ${}^0K_2$, and ${}^4K_2$ (Johnson et al., 1976):

$$\bar{X} = \sqrt[4]{\left[K_{44}^{-1}\,\frac{1 - {}^4f_2}{1 - {}^0f_2}\,\exp({}^0f_2 - {}^4f_2)\right]} \tag{9}$$

where

$${}^0f_2 = \frac{\sqrt{1 + 4[P_t]^0K_2} - 1}{2[Pt]^0K_2} \tag{10}$$

$${}^4f_2 = \frac{\sqrt{1 + 4[P_t]^4K_2} - 1}{2[P_t]^4K_2} \tag{11}$$

The fractions of dimers for the unliganded and fully liganded systems are designated by ${}^0f_2$ and ${}^4f_2$, respectively.

*Methods of Data Analysis.* The median ligand activity ordinarily can be determined by standard integration procedures such as planimetry or numerical integration. However, when oxygenation isotherms of CoHb are measured the macromolecule never reaches complete oxygen saturation even under 1 atm of $O_2$(g), and therefore, the median is less well determined and integration of the isotherm at the upper asymptote requires a model for extrapolation. The most accurate model for extrapolating the upper asymptote would in principle be the $O_2$-linked dimer–tetramer equation for $\bar{Y}$ (eq 8). However, in the absence of a priori knowledge of the thermodynamic parameters of the system this strategy was found to be unstable due to the lack of experimental information at high fractional saturation values. Therefore, the individual isotherms were fitted to third- and fourth-order $\bar{Y}$ functions as a more robust method to approximate upper asymptotes, and medians were calculated by numerical integration of the best-fit curve.

The ill-defined upper asymptote of the oxygenation isotherm of CoHb also posed a problem for normalizing raw absorbance data to the traditional functional form of the fitting equation, i.e., the fractional saturation, $\bar{Y}$. In order to avoid the likelihood of producing serious unknown bias and nonuniformity of experimental error into the fractional saturation domain, least-squares regression was performed on the raw absorbance data. Moreover, it was necessary to augment the analysis by simultaneously fitting the isotherms measured over a range of CoHb concentrations. The data were converted to $\bar{Y}$ values for representation purposes after regression.

Absorbance data, $A(X_i)$, were fitted to the equation:

$$A(X_i) = A_0 + (A_\infty - A_0)\bar{Y}(X_i) \tag{12}$$

where $X_i$ is the $O_2$ activity of the $i$th data point, $\bar{Y}(X_i)$ is the fractional saturation (eq 8) at $X_i$, and $A_0$ and $A_\infty$ are the asymptotic absorbance values for zero and infinite $O_2$ activities, respectively. The fractional saturation function, $\bar{Y}$, was reparameterized to fit for the parameters[3] $\Delta G_4$, ${}^0\Delta G_2$, ${}^1\Delta G_2$, ${}^3\Delta G_2$, ${}^4\Delta G_2$, $K_{coop2}$, and $\Delta G_{43}$. This formulation was previously found to decrease the correlation between fitting parameters in regression analysis of FeHb oxygenation data (Johnson et al., 1976). Equation 12 assumes that the observed absorbancies are directly proportional to the fractional saturation of the macromolecule. The sharp isosbestic condition for CoHb at intermediate saturation values (Imai et al., 1977) indicates this assumption is reasonable.

All nonlinear least-squares fitting was done with the program NONLIN from Dr. Michael L. Johnson (University of Virginia). The program employs a modified Gauss–Newton algorithm to find the most probable values of the adjustable parameters. Upper and lower confidence limits are evaluated by searching variance space for an $F$-statistic corresponding to 67% confidence probability and assumes the confidence intervals are asymmetric and correlated with other parameters

[2] For dimer cooperativity this simple relation for the average subunit assembly reaction of doubly ligated tetramers is not possible. Specific knowledge of the microscopic doubly ligated tetramer assembly free energies is required but is currently unavailable for oxygenation.

[3] The adjustable parameter $K_{coop2}$ allows for cooperativity within dissociated dimers and is defined as $K_{coop2} = k_{21}/2(k_{21}k_{22})^{1/2}$ (Mills et al., 1976).

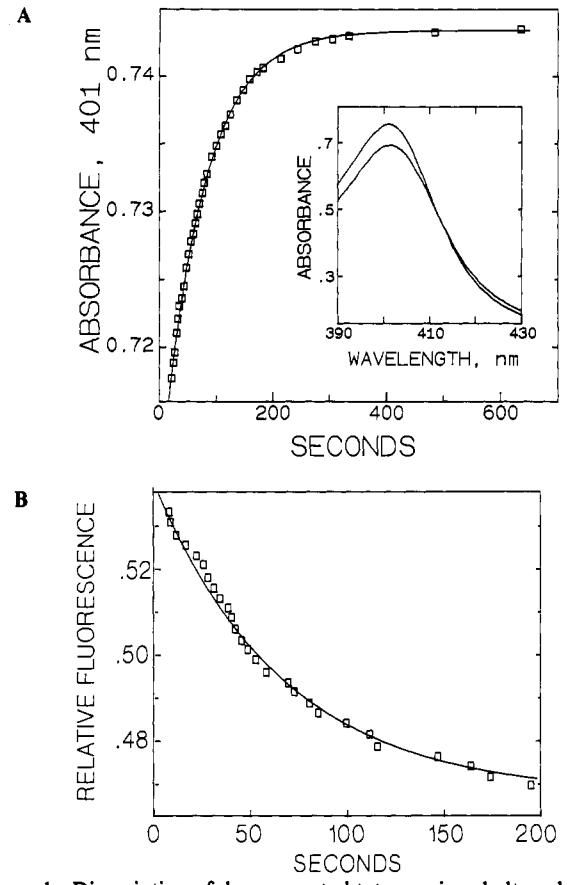


FIGURE 1: Dissociation of deoxygenated tetrameric cobaltous hemoglobin into dimers by haptoglobin quenching techniques. Reaction was monitored by (A) spectrophotometry at 401 nm (path length 1 cm), (B) fluorescence quenching above 310 nm with excitation at 280 nm (path length 0.1 cm). Inset to panel A shows spectra before (lower spectrum) and after mixing with haptoglobin. The solid curves are the best fits to eq 1 with a dissociation rate constant of 0.0150 (±0.0010) $s^{-1}$ (A) and 0.0150 (±0.0015) $s^{-1}$ (B). Solution conditions were as follows: approximately 1 $\mu$M monomer CoHb, 0.1 M Tris, 0.1 M NaCl (0.18 M total chloride), 1 mM $Na_2EDTA$, pH 7.40, 21.50 °C, and 0.01% sodium dithionite.

(Ackers et al., 1975; Johnson et al., 1976). Whenever asymmetric confidence limits were found, the largest error limit was reported (Table I) as a standard error.

## Results

*Dissociation Kinetics.* The inset to Figure 1A shows the spectral change in the Soret region of a solution of deoxygenated CoHb which has been completely dissociated into dimers and reacted with haptoglobin. The rate-limiting process for this reaction is the tetramer to dimer step, and the time course is shown in Figure 1A. Least-squares analysis of the data according to eq 1 gives a value for the dissociation rate constant $k_r$ = 0.0150 (±0.0010) $s^{-1}$ and an amplitude of 6.0% of the asymptotic absorbance. Since the dead time for mixing in the split-cell method is about 20 s, the reaction was also investigated by stopped-flow absorbance techniques and yielded the same rate constant (Speros, 1990).

Alternatively, the dissociation time course can be monitored as fluorescence quenching of the haptoglobin–dimer complex (Figure 1B). Regression analysis of the fluorescence dissociation kinetics data according to eq 1 yielded a dissociation rate constant of 0.0150 (±0.0015) $s^{-1}$ with an amplitude of 15.5% of the fluorescence emission. Attempts to include additional kinetic phases in the regression fitting equation for any of the dissociation experiments did not lead to statistical improvement.

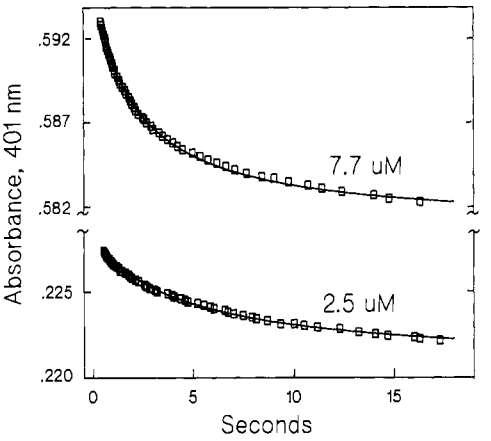


FIGURE 2: Reassociation of deoxygenated tetrameric cobaltous Hb from dimers upon rapid deoxygenation with sodium dithionite as monitored spectrophotometrically. Experiments were done at two Hb concentrations as labeled (micromolar CoHb monomer). Regression analysis of the data to eq 2 yielded a forward rate constant equal to 1.1 (±0.1) × $10^6$ $M^{-1}$ $s^{-1}$. Conditions were as follows: 0.1 M Tris, 0.1 M NaCl (0.18 M total chloride), 1 mM $Na_2EDTA$, pH 7.40, and 21.50 °C.

*Reassociation Kinetics.* The absorbance change upon rapid deoxygenation of a solution of CoHb is shown in Figure 2. During the first 1–2 s the data are largely attributable to removal of oxygen from the macromolecule and are therefore not shown. The remaining time course represents the association of deoxygenated dimers into tetramers and is well described by the rate law in eq 2. The forward rate constant determined by regression analysis of the data in Figure 2 is $k_f$ = 1.1 (±0.1) × $10^6$ $M^{-1}$ $s^{-1}$. This value is identical with the consensus value of $k_f$ = 1.1 (±0.3) × $10^6$ $M^{-1}$ $s^{-1}$ measured for mutant and normal human hemoglobins over a wide range of solution conditions (Pettigrew et al., 1982; Turner, 1989). The free energy for dimer–tetramer assembly of deoxygenated CoHb, calculated from the forward and reverse reaction rate constants, is equal to −10.6 (±0.1) kcal.

*Determination of* $^4\Delta G_2$. The equilibrium between fully oxygenated dimers and tetramers can be measured directly by analytical gel permeation chromatography for most chemically modified and mutant human hemoglobins. However, for cases where the macromolecular system is not completely saturated under 1 atm of $O_2$(g), the assembly equilibrium constant cannot be determined in such a straightforward manner. Alternatively, the equilibrium constant $^4\Delta G_2$ can be determined according to eq 9 by measuring medians of isotherms at different CoHb concentrations (Mills et al., 1976; Chu et al., 1984; Ackers & Johnson, 1990).

Figure 3 shows the logarithm of the median $O_2$ concentrations for CoHb over a range of concentration, along with the best-fit curve of the data to eq 9. Since the scatter in the medians is larger than has been observed with FeHb studies (for reasons described under Methods of Data Analysis), the potential problem of obtaining biased parameter estimates was alleviated by measuring 37 separate isotherms. The fully oxygenated dimer to tetramer assembly free energy thus determined is $^4\Delta G_2$ = −9.1 (±0.3) kcal, a value that represents stabilization of the tetramer by approximately 1 kcal relative to that of FeHb. The free energy for complete saturation of tetrameric CoHb was found to be $\Delta G_4$ = −20.84 (±0.07) kcal, compared to $\Delta G_4$ = −27.09 (±0.05) for FeHb (Chu et al., 1984).

The fitting procedure for determination of $^4\Delta G_2$ from isotherm medians did not require data over the full range of the curve shown in Figure 3 since $^0\Delta G_2$ was constrained by

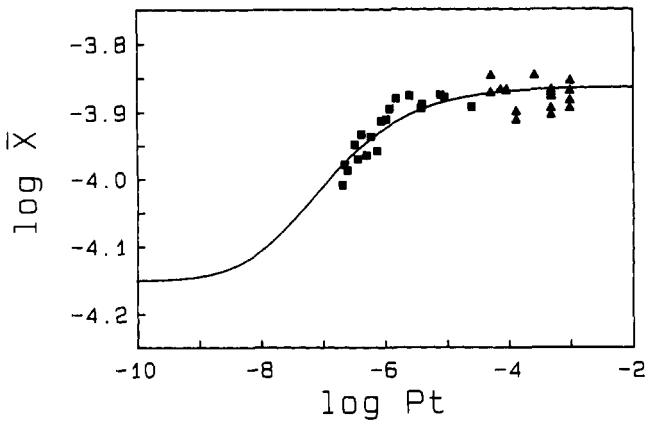


FIGURE 3: Logarithm of the median $O_2$ concentrations for oxygenation of cobaltous Hb as a function of the concentration of cobaltous hemoglobin [$P_t$] (monomer units). Squares represent data obtained with the Imai cell, and triangles were taken with the Gill cell. Solution conditions were as follows: 0.1 M Tris, 0.1 M NaCl (0.18 M total chloride), 1 mM $Na_2EDTA$, pH 7.40, and 21.50 °C. The curve is the best fit to eq 9.

methods described below. First, it should be noted that there is an interdependence between determinations of ${}^0\Delta G_2$ and ${}^4\Delta G_2$. The use of eq 2 for determination of $k_f$ (a component of ${}^0\Delta G_2$) requires knowledge of the initial dimer concentration $D_0$, calculated from ${}^4\Delta G_2$. Furthermore, it is not feasible to determine both ${}^0K_2$ and ${}^4K_2$ by eq 9 due to the lower limit of hemoglobin concentration at which isotherms can be measured. Hence the value of ${}^0K_2$ must be constrained in eq 9 in order to determine ${}^4K_2$ from a series of measured medians. In the present study the following strategy proved successful. An initial estimate for ${}^0\Delta G_2$ was obtained by using the consensus value for $k_f$ (above) and the independently measured value for $k_r$. The value of ${}^4\Delta G_2$ consequently determined from analysis of medians via eq 9 was then used to obtain an initial estimate of $D_0$ in the analysis of the reassociation kinetics data via eq 2. The ${}^4\Delta G_2$ determined from the intermediate analysis of isotherm data (below) then provided a final consistency test on analysis of the reassociation kinetics data according to eq 2. The extent of interdependence between these determinations depends to a large degree on the actual parameters of the system and the range of data collected. Regression analysis of the median data by eq 9 with a range of constrained values for ${}^0\Delta G_2$ showed that determinations of ${}^4\Delta G_2$ are effectively insensitive to the experimental error in determination of ${}^0\Delta G_2$. For example, perturbing ${}^0\Delta G_2$ by 5-fold greater than the standard deviation (i.e., ±0.5 kcal) led to best-fit values of ${}^4\Delta G_2$ which ranged only ±0.2 kcal. This robust feature of ${}^4\Delta G_2$ was crucial to the successful determination of accurate parameters in the cobalt system.

*Resolution of the Intermediate Ligation States.* The parameters of the linkage scheme, Scheme I, are determined by global fitting of isotherms measured over a range of CoHb concentration in combination with the value of ${}^0\Delta G_2$ measured independently. Eleven isotherms were selected from the total data set represented in Figure 3 solely on the basis of their close proximity to the best-fit median curve. The final data set was narrowed to eight isotherms after examination of residuals for preliminary fits. Figure 4 shows the results of analysis of the eight isotherms after converting the data to fractional saturation. Examination of the residuals (Figure 4) indicates the general correctness of the fitting equation and attests to the appropriatenes of the uniform weighting procedure employed during regression. The small nonrandom runs of residuals for individual isotherms may arise from manual digitization of the absorbance traces (see Materials

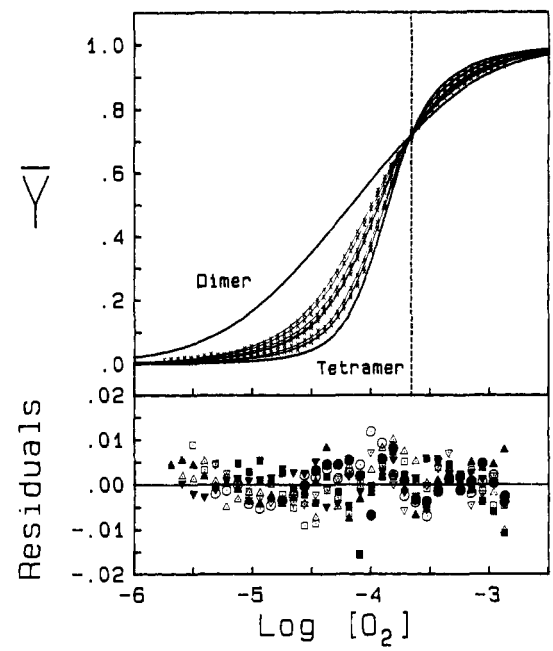


FIGURE 4: (Top) Oxygenation isotherms of CoHb at different Hb concentrations (0.22, 0.32, 0.59, 0.86, 1.0, 4.0, 7.8, and 9 μM in monomer units). Solution conditions: 0.1 M Tris, 0.1 M NaCl (0.18 M total chloride), 1 mM $Na_2EDTA$, pH 7.40, and 21.50 °C. Every other data point is shown as an (×). Smooth curves superposed with the data represent the best least-squares fit according to eq 12. The theoretical curves for $O_2$ binding to pure dimer and tetramer forms (as labeled) are also shown. All curves are normalized to fractional saturation for graphical representation. The dashed line demarcates the $O_2$ activity above which the tetramer exhibits quaternary enhancement relative to the dimer species. (Bottom) Residuals ($\bar{Y}$ units) for the simultaneous fit of the eight isotherms. Every fifth residual is plotted for clarity. The symbols correspond to CoHb concentrations (monomer units) of 0.22 μM (△); 0.32 μM (▽); 0.59 μM (⊡); 0.86 μM (⊙); 1.0 μM (▲); 4.0 μM (▼); 7.8 μM (■); and 9.0 μM (●). Isotherms of concentrations 4.0 μM or less were monitored at 422 nm, and the remaining data were collected at 570 nm.

and Methods). The best-fit parameters from the eight isotherms are summarized in Table I. The value of ${}^4\Delta G_2$ we report in the present study is that obtained by simultaneous analysis of the eight isotherms (Table I) since it is better resolved than that obtained by analysis of medians only. (The two agree within one standard deviation.)

The statistical significance of the dimer apparent anticooperativity (difference between $\Delta G'_{21}$ and $\Delta G'_{22}$ in Table I) was evaluated by comparing the variance of fit for the parameters in the table to the variance of fit where the dimer was constrained to be noncooperative. The ratio of the two variances (with $F$-statistic of 1.29) was used to test the null hypothesis against an $F$-distribution (Press et al., 1986). The improvement in the fit with dimer apparent anticooperativity was above the 98% probability level. Similar tests performed on FeHb oxygenation data showed no statistical improvement, consistent with previous FeHb oxygenation work (Mills et al., 1976; Chu et al., 1984).

## Discussion

*Overall Cooperative Free Energy, $\Delta G_c$.* The first objective of the present study was to determine the dimer–tetramer assembly free energy change for fully oxygenated CoHb, ${}^4\Delta G_2$. The principle motivation for this determination is that, in combination with the deoxygenated assembly free energy, ${}^0\Delta G_2$, the overall cooperative free energy, $\Delta G_c$, of tetrameric CoHb is given by (Ackers & Smith, 1987)

$$\Delta G_c \equiv {}^4\Delta G_2 - {}^0\Delta G_2 = \Delta G_4 - 2\Delta G_2 \qquad (13)$$

According to Scheme I and eq 13 $\Delta G_c$ represents the overall

Table I: Thermodynamic Parameters for the $O_2$-Linked Dimer–Tetramer Linkage System of Cobaltous Hemoglobin[a]

| parameter | macroscopic $\Delta G$ (kcal) | statistical term[b] | intrinsic $\Delta G'$ (kcal) |
|---|---|---|---|
| | Subunit Association Free Energies | | |
| ${}^0\Delta G_2$[c] | −10.6 ± 0.10 | $RT$ ln 1 | −10.6 ± 0.10 |
| ${}^1\Delta G_2$[d] | −9.12 ± 0.09 | $RT$ ln (1/2) | −8.71 ± 0.09 |
| ${}^3\Delta G_2$[d] | −8.69 ± 0.08 | $RT$ ln (1/2) | −8.28 ± 0.08 |
| ${}^4\Delta G_2$[d] | −8.76 ± 0.09 | $RT$ ln 1 | −8.76 ± 0.09 |
| | Changes in Intersubunit Contact Free Energies[e] | | |
| $\delta\Delta G_{01}$ | 1.48 ± 0.13 | $RT$ ln (1/2) | 1.89 ± 0.13 |
| $\delta\Delta G_{13}$ | 0.43 ± 0.12 | $RT$ ln 1 | 0.43 ± 0.12 |
| $\delta\Delta G_{34}$ | −0.07 ± 0.12 | $RT$ ln 2 | −0.48 ± 0.12 |
| | Dimer Oxygen Binding Free Energies | | |
| $\Delta G_{21}$[f] | −6.27 ± 0.10 | $RT$ ln (1/2) | −5.86 ± 0.10 |
| $\Delta G_{22}$[f] | −4.96 ± 0.13 | $RT$ ln 2 | −5.37 ± 0.13 |
| $\Delta G_2$ | −11.23 ± 0.08 | $RT$ ln 1 | −11.23 ± 0.08 |
| | Tetramer Oxygen Binding Free Energies | | |
| $\Delta G_{41}$ | −4.79 ± 0.17 | $RT$ ln (1/4) | −3.98 ± 0.17 |
| $\Delta G_{42}$ | −5.22 ± 0.34 | $RT$ ln (2/3) | −4.98 ± 0.34 |
| $\Delta G_{43}$[d] | −5.57 ± 0.21 | $RT$ ln (3/2) | −5.81 ± 0.21 |
| $\Delta G_{44}$ | −5.03 ± 0.21 | $RT$ ln 4 | −5.84 ± 0.21 |
| $\Delta G_4$[d] | −20.61 ± 0.04 | $RT$ ln 1 | −20.61 ± 0.04 |

[a] Solution conditions: 0.1 M Tris, 0.1 M NaCl, 1 mM $Na_2EDTA$, pH 7.40, and 21.50 °C. Free energy changes are in kilocalories. The square root of the variance for the global fit to eight isotherms was 0.004 in $\bar{Y}$ units with 1087 degrees of freedom. [b] These corrections (in calories) for statistical degeneracies are subtracted from the macroscopic free energy changes to yield the intrinsic values. [c] Constrained during regression analysis. [d] Adjustable parameters. Confidence intervals were essentially symmetric about the tabulated most probable values. Confidence intervals were essentially symmetric about the tabulated most probable values. Confidence limits for the remaining parameters were propagated [cf. Bevington, (1969)]. [e] Calculated as $\delta\Delta G_{ij} = {}^j\Delta G_2 - {}^i\Delta G_2$. [f] The term $K_{coop2}$ (see Methods of Data Analysis) was an adjustable parameter which allows for dimer cooperativity. The best-fit value was $K_{coop2} = 1.52 \pm 0.14$.

Table II: Overall Cooperativity and Subunit Assembly Gibbs Free Energy Changes for Three Hemoglobin Ligation Systems[a]

| system | ${}^4\Delta G_2$ (kcal) | ${}^0\Delta G_2$ (kcal)[b] | $\Delta G_c$ (kcal) |
|---|---|---|---|
| FeHb/$O_2$[c] | −8.05 ± 0.1 | −14.35 ± 0.1 | 6.30 ± 0.14 |
| CoHb/$O_2$ | −8.76 ± 0.09 | −10.6 ± 0.1 | 1.84 ± 0.13 |
| CoHb/Fe–CO[d] | −8.0 ± 0.1 | −10.6 ± 0.1 | 2.60 ± 0.14 |

[a] Solution conditions: 0.1 M Tris, 0.1 M NaCl, 1 mM $Na_2EDTA$, pH 7.40, and 21.50 °C. Parameters are defined in Scheme I and eq 13. [b] From kinetic measurements (see text). [c] Chu et al., 1984. [d] Speros et al., 1991.

free energy of cooperativity originating from dimer–dimer subunit interactions which is used to regulate oxygen affinity. Table II lists $\Delta G_c$ for the three ligation systems. The value of 1.84 found here for the CoHb/$O_2$ system is considerably lower than the value of 6.3 for FeHb/$O_2$ and originates largely in the 3.75-kcal destabilization of the deoxygenated tetramer form. The effect that this reduced value of $\Delta G_c$ has on oxygen binding cooperativity depends on how it is distributed among the intermediate binding steps.

Molecular-level interpretation of experimental solution properties of hemoglobin relies critically on knowledge of the fraction of dimer and tetramer forms present. These fractions can be calculated from ${}^0\Delta G_2$ and ${}^4\Delta G_2$ with eqs 10 and 11. Figure 5 depicts the fraction of dimer species for fully oxygenated and unliganded CoHb and FeHb over a range of typical experimental concentrations. The figure shows that the fully oxygenated CoHb tetramer is stabilized relative to FeHb, while the deoxygenated CoHb tetramer is destabilized. Table II summarizes the dimer–tetramer assembly free energy changes and overall cooperativity terms for the three macromolecule ligation systems.

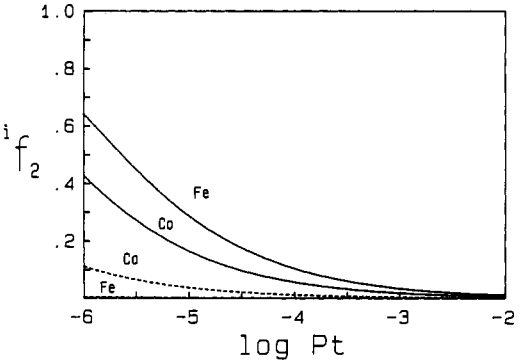


FIGURE 5: Fraction of CoHb and FeHb as the dimer form for the deoxygenated (dashed curves) or fully oxygenated (solid curves) ligation state as a function of the total Hb concentration (monomer units). The curves are from eqs 10 and 11 based on the values of ${}^0\Delta G_2$ and ${}^4\Delta G_2$ listed in Table II. Solution conditions: 0.1 M Tris, 0.1 M NaCl (0.18 M total chloride), 1 mM $Na_2EDTA$, pH 7.40, and 21.50 °C.

*Intermediate Oxygenation Properties of CoHb Dimers.* Comparison of the first and second stepwise intrinsic free energies for $O_2$ binding to the dimers (Table I) shows that $\Delta G'_{22} - \Delta G'_{21} = 0.49$ (±0.16) kcal of apparent anticooperativity. Mechanistically, the apparent anticooperativity could arise from different $O_2$ binding affinities of the $\alpha$ and $\beta$ subunits, by energetically unfavorable interactions moderated by the protein, or from a combination of both.

*Intermediate Oxygenation Properties of CoHb Tetramers.* The pattern of intrinsic free energy changes for sequential oxygenation of tetrameric CoHb (Table I) indicates that the molecule undergoes cooperative transitions during the second and third ligation steps, releasing about 1 kcal of quaternary constraint at each step, while the oxygen binding reaction at the last step is noncooperative (i.e., the intrinsic free energy changes at the last two ligation steps are essentially equal). Previous work (Imai et al., 1977) at 15 °C which assumed only tetrameric molecules in a solution of 60 $\mu$M CoHb (monomer units) indicated a similar pattern of cooperativity except no cooperativity was observed at the second step. The temperature dependence of CoHb oxygenation (Ikeda-Saito & Verzili, 1981) at 120 $\mu$M subunit concentration predicts cooperativity at the second step (about 0.16 kcal) at 22 °C. Despite differences found under different conditions and using different experimental strategies, the qualitative findings of decreased steepness in the oxygenation isotherm of CoHb are seen in all studies.

Cooperativity measured as the steepness of the ligand binding curve has traditionally been quantified as the slope of the Hill plot [cf. Edsall and Gutfreund (1983)]. Figure 6A compares the Hill slope as a function of saturation for three Hb ligation systems. The steepness of the FeHb/$O_2$ system is clearly much greater than for the two cobalt systems, especially at high degrees of saturation. The three dashed lines for the CoHb/Fe–CO system[4] represent the range of values

[4] The Hill slope curves for CoHb/Fe–CO were calculated from cooperative free energies (Speros et al., 1991). The following equation was used to calculate tetrameric Adair constants:

$$K_{4i} = \sum_j {}^{ij}k_\alpha'^p\, {}^{ij}k_\beta'^q\, g^{ij} \exp\left[-\left(\frac{{}^{ij}\Delta G_2 - {}^{01}\Delta G_2 + n_{ij}\Delta G_{\alpha\beta}}{RT}\right)\right]$$

Here ${}^{ij}k_\alpha'^q$ and ${}^{ij}k_\beta'^s$ are the intrinsic $O_2$ affinity equilibrium constants of the $\alpha$ and $\beta$ subunits in the $\alpha\beta$ dimer, $\Delta G_{\alpha\beta}$ allows for possible site–site cooperativity between the $\alpha\beta$ subunits in the dimer, and ${}^{ij}\Delta G_2$ is the subunit assembly free energy for the $j$th microstate of the $i$th ligation state. Values of the statistical degeneracy $g^{ij}$ and the notational terms $p$, $q$, and $n_{ij}$ are in Table III.

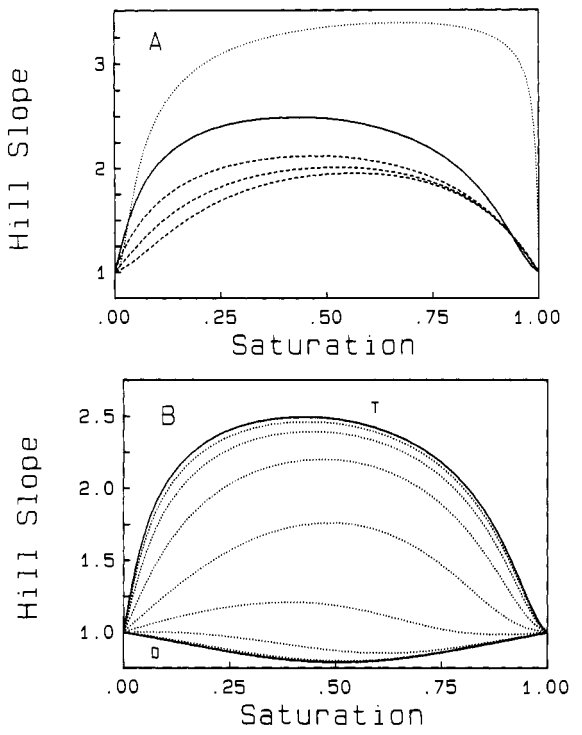


FIGURE 6: Slope of the Hill plot versus fractional saturation of tetrameric Hb. (A) Three Hb ligation systems are presented: CoHb/$O_2$ (present study, solid curve); FeHb/$O_2$ (Chu et al., 1984; dotted line); and CoHb/Fe–CO (Speros et al., 1991; dashed lines). The three curves for CoHb/Fe–CO represent the range of mechanisms that could explain the observed dimer anticooperativity allowed to exist (see text). The maximum Hill slopes are as follows: CoHb/$O_2$, 2.49; FeHb/$O_2$, 3.38; and CoHb/Fe–CO, 2.12, 2.01, and 1.95. (B) Hill slope for the CoHb/$O_2$ system at various concentrations of CoHb. The curves for the pure tetramer (top) and dimer (bottom) are shown as solid curves. Dotted curves from top to bottom are as follows (monomer units): 1 mM, 100 $\mu$M, 10 $\mu$M, 1 $\mu$M, 100 nM, 10 nM, and 1 nM. Solution conditions: 0.1 M Tris, 0.1 M NaCl (0.18 M total chloride), 1 mM $Na_2EDTA$, pH 7.40, and 21.50 °C.

Table III: Statistical and Notational Terms Employed To Calculate Tetrameric Adair Equilibrium Constants from the Microstate Cooperative Free Energies of the CoHb/Fe–CO Ligation System

| $ij$[a] | $p$ | $q$ | $n_{ij}$ | $g_{ij}$ |
|---|---|---|---|---|
| 0 1 | 0 | 0 | 0 | 1 |
| 1 1 | 1 | 0 | 0 | 2 |
| 1 2 | 0 | 1 | 0 | 2 |
| 2 1 | 1 | 1 | 1 | 2 |
| 2 2 | 1 | 1 | 0 | 2 |
| 2 3 | 2 | 0 | 0 | 1 |
| 2 4 | 0 | 2 | 0 | 1 |
| 3 1 | 1 | 2 | 1 | 2 |
| 3 2 | 2 | 1 | 1 | 2 |
| 4 1 | 2 | 2 | 2 | 1 |

[a] See preceding paper (Speros et al., 1991) for definition of the $ij$ microstates.

for $k'_\alpha$, $k'_\beta$, and $\Delta G_{\alpha\beta}$, which could explain the 0.49 kcal of dimer apparent anticooperativity found for the oxygenation studies of the CoHb/$O_2$ system and are therefore presented as a formal possibility. (The $\alpha$ chains have either higher or lower $O_2$ affinity than the $\beta$ chains in the $\alpha\beta$ dimer, or both chain types have identical $O_2$ affinity but with site–site cooperativity of 0.49 kcal.)

Figure 6B shows the Hill slope for $O_2$ binding to CoHb at various concentrations of CoHb. The steepest Hill slope, pertaining to the pure tetramer state ($n_{max}$ = 2.49), is approached at concentrations above 1 mM. Hill slope values less than unity at very low concentrations originate from apparent anticooperativity in the CoHb $\alpha\beta$ dimers.

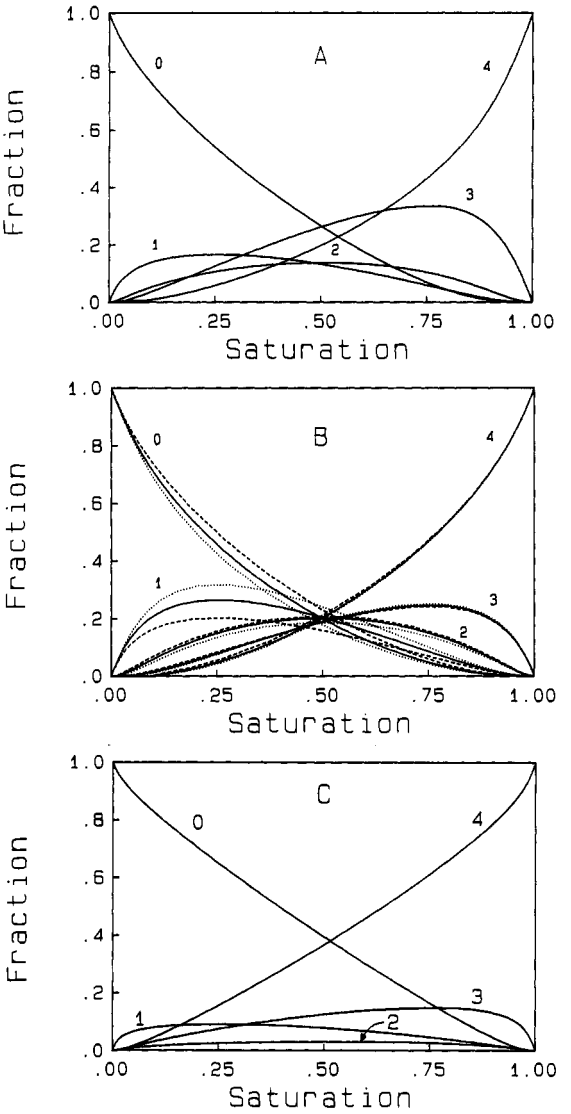


FIGURE 7: Fractional population of macroscopic ligation species of tetrameric Hb: CoHb/$O_2$ (present study) (A); CoHb/Fe–CO (Speros et al., 1991) (B); and FeHb/$O_2$ (Chu et al., 1984) (C). The three sets of curves for the CoHb/Fe–CO system represent the range of different possibilities for the apparent dimer anticooperativity (see text). Solution conditions: 0.1 M Tris, 0.1 M NaCl (0.18 M total chloride), 1 mM $Na_2EDTA$, 21.50 °C, and pH 7.40 (A and B) and pH 9.50 (C).

The relative populations of intermediate ligation states reflect the underlying cooperative mechanism, and such population "maps" (Figure 7) serve as key diagnostic tools in addressing mechanistic issues. The generally large values of Hill slope (Figure 6A) for FeHb/$O_2$ translate into the well-known suppressed levels of populations of the intermediate ligation states (Figure 7C). Likewise, the smaller Hill slopes seen for the CoHb systems correspond to somewhat elevated levels of the populations of intermediate states (Figure 7A,B). Comparison of the relative populations of species for the two CoHb ligation systems shows great similarities, particularly with regard to the elevated levels of triply ligated states. Moreover, both mimic the distribution of oxygenated species observed with $HbA_0$ at high pH shown in Figure 7C. These similarities suggest a common underlying mechanism which can be modulated by proton activity and the nature of the heme-site ligand.

*Coupling between Oxygenation and Intermediate Subunit Assembly Reactions.* A direct measure of the subunit–subunit energetics that regulate oxygen affinity is given by the in-

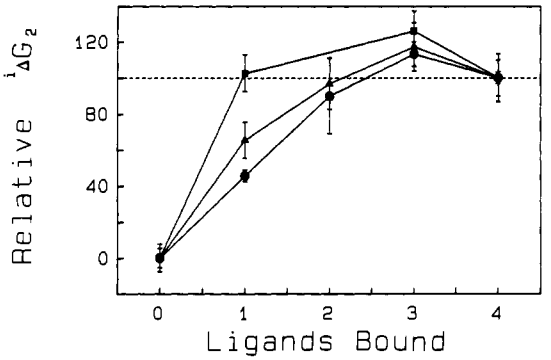


FIGURE 8: Relative dimer–tetramer subunit assembly free energy changes versus the *i*th ligation state of the tetramer for three Hb ligation systems: CoHb/$O_2$ (present study) (■); CoHb/Fe–CO (Speros et al., 1991) (▲); and FeHb/$O_2$ (Chu et al., 1984) (●). Relative values were calculated as $100 \times [(^{i}\Delta G_2 - {}^{0}\Delta G_2)/\Delta G_c]$. Error bars are for ±1 standard deviation and are plotted symmetrically about each point. Assembly free energy changes which are above the dashed line correspond to values where quaternary enhancement occurs relative to the fully liganded state. Solution conditions were as follows: 0.1 M Tris, 0.1 M NaCl (0.18 M total chloride), 1 mM $Na_2EDTA$, pH 7.40, and 21.50 °C.

termediate subunit assembly free energies (Scheme I). Two lines of evidence indicate that most of the cooperativity-linked intersubunit interactions are given by these assembly free energies, i.e., that regulatory interactions occur largely across the $\alpha_1\beta_1$–$\alpha_2\beta_2$ interface rather than between $\alpha$ and $\beta$ chains of the $\alpha\beta$ dimer. First, oxygenation studies over a range of conditions show no cooperativity within the dissociated dimers (Mills et al., 1976; Mills & Ackers, 1979a; Chu et al., 1984). Second, crystallographic analysis of deoxy- and oxy-FeHb does not reveal significant structural changes at the $\alpha_1\beta_1$ interface (Baldwin & Chothia, 1979).

Figure 8 displays the relationship between ligation and quaternary switching events. The largest change in subunit assembly interaction of the CoHb oxygenation system is seen to occur at the first ligation step. It is noteworthy that cooperative processes that occur concurrent with the first ligation event are transparent to traditional Adair analysis of the tetrameric $O_2$ binding isotherm alone (i.e., knowledge only of the four stepwise free energy changes $\Delta G_{4i}$, $i = 1$–4). The additional knowledge of ligand-linked subunit assembly free energies thus provides valuable mechanistic knowledge that is normally unavailable.

Since the doubly ligated subunit assembly reaction for the CoHb/$O_2$ system cannot currently be calculated for the case of anticooperative dimers (footnote 2 under Theory), one cannot evaluate the changes in subunit interaction at this ligation state. However, one can assess the change in subunit assembly free energy in going from the singly to the triply ligated form. As shown in Figure 8, there is a release of quaternary constraint energy ($\delta\Delta G'_{13} = 0.43$ (±0.12) kcal from Table I) in going from the singly to the triply ligated state for all three ligation systems.

The last $O_2$ binding step of tetrameric CoHb is noncooperative on the basis of evaluation of the intrinsic free energy changes for the third and fourth ligation steps. However, additional knowledge from subunit assembly free energies shows that 0.48 (±0.12) kcal of quaternary enhancement energy is gained in the $O_2$ affinity (Table I, $\delta\Delta G'_{34}$). As a result, the $O_2$ affinity of the last binding step to the tetramer is greater than that of the last step to the dimer. Indeed, one can clearly see this effect from the isotherm data in Figure 4, where for all $O_2$ activities above the dashed line the tetramer has the higher $O_2$ affinity. Quaternary enhancement has been found for oxygenation of FeHb under a variety of conditions (Mills & Ackers, 1979ab; Chu et al., 1984), and in the microstate distribution of the CoHb/Fe–CO system (Speros et al., 1991). The ability of tetrameric hemoglobin to enhance its oxygen affinity relative to the dissociated dimer state points to an important component of its cooperative mechanism [see Ackers and Johnson (1990) for a recent review].

*Concluding Remarks.* Structural perturbation at the heme site of human hemoglobin by substitution of Fe(II) by Co(II) is found to have several functional consequences including the following: the total cooperative free energy is reduced from 6.30 (±0.14) to 1.84 (±0.13) kcal; the dimer is found to exhibit an apparent anticooperativity of 0.49 (±0.16) kcal, whereas FeHb dimers bind $O_2$ noncooperatively (Chu et al., 1984); and the steepness of the tetrameric $O_2$ binding isotherm is reduced (maximum Hill slope is 2.49 versus 3.38 for FeHb). In contrast, comparison of the linkage energetics of the CoHb/$O_2$ and CoHb/Fe-CO systems shows remarkable similarities and demonstrates that the ligand analogue Fe–CO is a useful model for the reversible ligand $O_2$. The covalent ligand analogue Fe–CO has powerful utility in allowing configurational isomers of the various ligation states to be studied in isolation (Speros et al., 1991) in contrast to oxygen which rearranges rapidly among different binding sites.

Despite minor differences in functional behavior of the CoHb/$O_2$, CoHb/Fe–CO, and FeHb/$O_2$ ligation systems, important mechanistic properties of these systems are maintained. In all three systems cooperativity is achieved by the release of quaternary constraints at low saturations and the gain of quaternary enhancement free energy at the last ligation step. Moreover, the relative populations of the intermediate ligation states for all three systems indicate that the fundamental mechanism of cooperativity is the same.

**Registry No.** $O_2$, 7782-44-7.

## REFERENCES


Ackers, G. K., & Halvorson, H. R. (1974) *Proc. Natl. Acad. Sci. U.S.A. 91*, 4312–4316.

Ackers, G. K., & Smith, F. R. (1987) *Annu. Rev. Biophys. Biophys. Chem. 16*, 583–609.

Ackers, G. K., & Johnson, M. L. (1990) *Biophys. Chem. 37*, 265–279.

Ackers, G. K., Johnson, M. L., Mills, F. C., Halvorson, H. R., & Shapiro, S. (1975) *Biochemistry 14*, 5128–5134.

Atha, D. H., Johnson, M. L., & Riggs, A. F. (1979) *J. Biol. Chem. 254* (24), 12390–12398.

Baldwin, J., & Chothia, C. (1979) *J. Mol. Biol. 129*, 175–220.

Bevington, P. R. (1969) in *Data Reduction and Error Analysis for the Physical Sciences*, McGraw-Hill, New York.

Chu, A. H., Turner, B. W., & Ackers, G. K. (1984) *Biochemistry 23*, 604–617.

Connell, G. E., & Shaw, R. W. (1961) *Can. J. Biochem. Physiol. 31*, 1013–1019.

Dolman, D., & Gill, S. J. (1978) *Anal. Biochem. 87*, 127–134.

Doyle, M. L., Simmons, J. H., & Gill, S. J. (1990) *Biopolymers 29*, 1129–1135.

Edsall, J. T., & Gutfreund, H. (1983) in *Biothermodynamics: The Study of Biochemical Processes at Equilibrium*, Wiley & Sons, New York.

Haupt, G. W. (1952) *J. Opt. Soc. Am. 42*, 441–447.

Hoffman, B. M., & Petering, D. H. (1970) *Proc. Natl. Acad. Sci. U.S.A. 67* (2), 637–643.

Hwang, P. K., & Greer, J. (1980) *J. Biol. Chem. 255*, 3038–3041.

Ikeda-Saito, M., & Verzili, D. (1981) *J. Mol. Biol. 153*, 441–449.

Imai, K. (1978) in *Allosteric effects in haemoglobin*, Cambridge University Press, Cambridge, U.K.
Imai, K., Yonetani, T., & Ikeda-Saito, M. (1977) *J. Biol. Chem. 109*, 83-97.
Ip, S. H. C., Johnson, M. L., & Ackers, G. K. (1976) *Biochemistry 15*, 654-660.
Johnson, M. L., Halvorson, H. R., & Ackers, G. K. (1976) *Biochemistry 15*, 5363-5371.
Mills, F. C., & Ackers, G. K. (1979a) *J. Biol. Chem. 254* (8), 2881-2887.
Mills, F. C., & Ackers, G. K. (1979b) *Proc. Natl. Acad. Sci. U.S.A. 76* (1), 273-277.
Mills, F. C., Johnson, M. L., & Ackers, G. K. (1976) *Biochemistry 15*, 5350-5362.
Nagel, R. L., & Gibson, Q. H. (1971) *Biochemistry 10*, 69.
Pettigrew, D. W., Romeo, P. H., Tsapis, A., Thillet, J., Smith, M. L., Turner, B. W., & Ackers, G. K. (1982) *Proc. Natl. Acad. Sci. U.S.A. 79*, 1849-1853.
Press, W. H., Flannery, B. P., Teukolsky, S. A., & Vetterling, W. T. (1986) in *Numerical Recipes: The Art of Scientific Computing*, p 468, Cambridge University Press, Cambridge.
Speros, P. C. (1990) Ph.D. Dissertation, The Johns Hopkins University.
Speros, P. C., LiCata, V. J., Yonetani, T., & Ackers, G. K. (1991) *Biochemistry* (preceding paper in this issue).
Turner, B. W. (1984) Ph.D. Dissertation, The Johns Hopkins University.
Turner, B. W., Pettigrew, D. W., & Ackers, G. K. (1981) *Methods Enzymol. 76*, 596-628.
Turner, G. J. (1989) Ph.D. Dissertation, The Johns Hopkins University.
Wyman, J., & Gill, S. J. (1990) in *Binding and Linkage: Functional Chemistry of Biological Macromolecules*, University Science Books, Mill Valley, CA.

# A Fluorescence Lifetime Study of Virginiamycin S Using Multifrequency Phase Fluorometry†

Koen Clays,‡ Mario Di Giambattista,§ Andre Persoons,‡ and Yves Engelborghs*,‡

*Laboratory of Chemical and Biological Dynamics, University of Leuven, Celestijnenlaan 200 D, B-3001 Leuven, Belgium, and Microbiology and Genetics Unit, Institute of Cellular Pathology, University of Louvain Medical School, B-1200 Brussels, Belgium*

*Received November 26, 1990; Revised Manuscript Received March 7, 1991*

ABSTRACT: Using multifrequency phase fluorometry, fluorescence lifetimes have been assigned to the different protolytic forms of the antibiotic virginiamycin S. These lifetimes are 0.476 ± 0.005 ns for the uncharged form, 1.28 ± 0.2 and 7.4 ± 0.2 ns for the zwitterionic form, 1.19 ± 0.01 ns for the negatively charged form, and 1.9 ± 0.1 ns for the double negatively charged form. The assignments are based on lifetime measurements as a function of pH, volume percent ethanol, and excitation wavelength. Excited-state proton transfer is taken into account. It is complete at pH values lower than 1, and no fluorescence of the fully protonated charged form is observed. At pH 8, an excited-state p$K^*$ increase is calculated, but proton association is too slow to cause excited-state proton transfer. The addition of divalent cations, at pH 9.4, increases the lifetime of the negatively charged form to a value dependent upon the specific nature of the cation (7.58 ± 0.06 ns for $Mg^{2+}$, 6.54 ± 0.02 ns for $Ca^{2+}$, and 3.74 ± 0.05 ns for $Ba^{2+}$). Monovalent cations do not influence the lifetimes, indicating that their binding to the macrocycle does not influence the fluorescent moiety. The model compound 3-hydroxypicolinamide shows an analogous behavior, but the retrieved lifetime can differ significantly.

Virginiamycin S (VS)[1] is a hexapeptide with a fluorescent side group (the 3-hydroxypicolinyl group) attached to it through an amide bond. It is an antibiotic because it blocks protein synthesis at bacterial ribosomes (Cocito, 1979). Due to a strong enhancement of the fluorescence of VS upon binding to ribosomes, its binding kinetics could be studied extensively by fluorescence stopped-flow techniques (Moureau et al., 1983; Di Giambattista et al., 1987). Its dissociation rate constant was obtained by displacement studies with erythromycin. Several other antibiotics show partial or complete overlap of their binding site with that of VS, such that their binding could also be studied, using displacement or competition kinetics. In this way, three partially overlapping binding sites could be discerned (Di Giambattista et al., 1987).

VS is only weakly fluorescent in aqueous solutions, but the fluorescence increases strongly in the presence of $Mg^{2+}$ ions. A further intensity increase is observed upon binding to the ribosomes. Responsible for this fluorescence is the 3-hydroxypicolinyl moiety. Quenching studies have shown that this group is buried in the ribosome complex and partially shielded from solvent access (Di Giambattista et al., 1984).

In this paper, a fluorescence lifetime study is described, using multifrequency phase fluorometry. The hydroxypicolinyl group appears in several protolytic forms, and the lifetimes were therefore determined as a function of pH, of the presence of $Mg^{2+}$ ions and ethanol. A comparison between VS and 3-

† K.C. is a research associate and Y.E. is research director of the Belgian National Fund for Scientific Research. Financial support was obtained from the Research Fund of the University of Leuven and from the Belgian National Fund for Scientific Research.

* Correspondence should be addressed to this author.
‡ University of Leuven.
§ University of Louvain Medical School.

[1] Abbreviations: VS, virginiamycin S; 3-HPA, 3-hydroxypicolinamide; SAS, species-associated spectrum.

0006-2960/91/0430-7271$02.50/0 